Cell Division

RESEARCH

Open Access

STEAP4 with copper reductase activity suppresses tumorigenesis by regulating the cell cycle in hepatocellular carcinoma cells

Ting Yang[1†], Minhong Zou[2†], Yujie Xie[1], Yong Zhang[1*], Kun Wang[3*], Shihai Jiang[4*] and Qiong Zou[1*]

Abstract

Background Abnormal expression of six-transmembrane epithelial antigen of prostate 4 (*STEAP4*) has been implicated in the carcinogenesis of hepatocellular carcinoma (HCC). However, the biological role and regulatory mechanisms of *STEAP4* in HCC remain unclear.

Methods and Results Here, we analyzed *STEAP4* expression levels and differentially expressed genes (DEGs) between *STEAP4* high- and low-expression groups using multiple databases. Proliferation assays, 5-ethynyl-2′-deoxyuridine (EdU) assays, propidium iodide (PI) flow cytometry, and colony formation assays were conducted to assess the effects of STEAP4 on HCC cell proliferation, cell cycle progression, and clonogenic capacity. STEAP4 was downregulated in HCC tumor tissues, with lower expression associated with poorer overall survival (OS) and disease-free survival (DFS) in patients. Functional network analysis suggested that *STEAP4* regulates cell cycle signaling, with tumor sections showing a negative correlation between STEAP4 and cell cycle proteins. Overexpression of STEAP4, combined with non-cytotoxic copper exposure in the HepG2 cell line, reduced proliferation and clonogenicity, induced cell cycle arrest, and downregulated the mRNA and protein levels of cell cycle-regulating genes. A predictive model based on *STEAP4* and cell cycle gene demonstrated prognostic value in HCC patients.

Conclusions Our results lay a foundation for further study of the cell cycle regulatory role of STEAP4 with Cu^{2+} reductase activity in HCC, indicating that STEAP4 may be a promising therapeutic target for HCC.

Keywords STEAP4, Hepatocellular carcinoma, Copper reductase activity, Cell cycle, Tumorigenesis

†Ting Yang and Minhong Zou have contributed equally to this work.

*Correspondence:
Yong Zhang
zhangyn9@mail.sysu.edu.cn
Kun Wang
wangk@mail.sysu.edu.cn
Shihai Jiang
Shihai.Jiang@medizin.uni-leipzig.de
Qiong Zou
zouqiong3@mail.sysu.edu.cn
[1] Department of Nuclear Medicine, Third Affiliated Hospital of Sun Yat-sen University, Guang Zhou 510630, Guangdong, China
[2] Department of Ultrasonic Diagnosis, Third Affiliated Hospital of Sun Yat-sen University, Guang Zhou 510630, Guangdong, China
[3] Department of Joint Surgery and Orthopedic Trauma, Third Affiliated Hospital of Sun Yat-sen University, Guang Zhou 510630, Guangdong, China
[4] Institute of Laboratory Medicine, Clinical Chemistry and Molecular Diagnostics, University Hospital Leipzig, 04103 Leipzig, Germany

Introduction

Hepatocellular carcinoma (HCC) is the most prevalent form of liver cancer, characterized by its aggressive nature and poor prognosis. Despite advances in diagnostics and treatment, HCC remains one of the leading causes of cancer-related mortality worldwide [1, 2]. The five-year survival rate for advanced HCC is low, mainly due to high recurrence and metastasis rates [3]. The lack of tumor type- or stage-specific molecular markers presents a critical barrier to improving HCC understanding and treatment [4]. Thus, identifying novel biomarkers and therapeutic targets is urgently needed to enhance patient outcomes.

The six-transmembrane epithelial antigen of the prostate (STEAP) family has attracted significant interest in oncology for its multifaceted roles in tumorigenesis and cancer progression. Initially recognized for high expression in prostate cancer, emerging evidence suggests that STEAP proteins, particularly STEAP4, may also play regulatory roles in liver cancer, including HCC [5–9]. The *STEAP4* (also known as STAMP2 and TIARP) is involved in copper reduction and transport [10]. Previous studies suggest that *STEAP4* is broadly expressed in various tissues [10–12] and has associations with obesity, insulin resistance, inflammation, and cancer progression [13–16]. Notably, *STEAP4* expression is dysregulated in multiple cancers, suggesting a role in tumorigenesis [15, 17–19]. Recent studies implicate STEAP4 as a potential prognostic marker in HCC, with Tang et al. demonstrating reduced *STEAP4* mRNA levels in HCC tissues compared to non-tumorous tissues and linking lower expression to advanced tumor stage and poorer survival rates [20]. These findings suggest that *STEAP4* could serve as a prognostic indicator in HCC, supporting risk stratification and treatment decision-making. Additionally, STEAP4 may influence cell proliferation and survival pathways, potentially hindering HCC progression. It has been shown to inhibit cisplatin resistance by suppressing the PI3K/AKT pathway, crucial in HCC growth and chemotherapy resistance [21]. However, the exact mechanisms of STEAP4 in HCC progression remain to be fully elucidated.

Dysregulated cell-cycle proteins are central to all cancer types and drive tumorigenesis [22]. Targeting cell-cycle kinases is a promising cancer therapeutic approach. The STEAP family has been implicated in cell-cycle regulation. Antibody blockade of STEAP4 was shown to inhibit pre-adipocyte proliferation via cell-cycle control [13], and STEAP1 is closely linked to carcinoma cell cycles [23]. Importantly, STEAP4 expression in HCC patients has been associated with response to immune checkpoint inhibitors [24], highlighting cell-cycle control as a likely regulatory mechanism for STEAP4 in cancer cells. Nonetheless, STEAP4's role in HCC cell-cycle regulation remains poorly understood.

As a family, STEAP proteins share metalloreductase activity, underscoring their significance in cancer metal metabolism [12]. Recent findings indicate that STEAP2 promotes HCC progression by increasing intracellular copper levels [25], while copper (I) compounds have demonstrated efficacy against human tumors by inducing cell-cycle arrest [26]. In addition, Copper (II)-modified molecules similarly induce oxidative stress and cell-cycle inhibition in tumor cells [27, 28]. However, non-cytotoxic copper overload can interact with mitochondrial metabolism to enhance cell proliferation [29], mainly through driving remodeling of metabolic state and bioenergetic benefits to promote cancer growth [30], suggesting that copper's role in cell-cycle regulation depends on its cellular concentration and reduction state [31]. Although STEAP4 is known for its copper reduction and transport functions, its copper reductase activity and possible involvement in cell-cycle regulation remain largely unexplored.

In this study, we examined *STEAP4* expression in HCC patients using public RNA-seq data, screened key genes in its functional network, and identified relationships between *STEAP4* expression and cell-cycle-related genes. We further evaluated the effects of STEAP4 overexpression, alongside non-cytotoxic copper exposure, on HCC cell proliferation, clonogenicity, and cell-cycle gene regulation *in- vitro*. Our findings suggest that STEAP4, in conjunction with its copper reductase activity, may offer prognostic value in HCC tumorigenesis and could provide insights for future therapeutic targets.

Results

Decreased *STEAP4* expression in hepatocellular carcinoma cohorts

STEAP4 mRNA expression was significantly downregulated in tumor tissues across multiple HCC cohorts (Fig. 1A, B). To confirm STEAP4 expression in HCC tissues, we conducted immunohistochemistry staining on twenty HCC and adjacent normal tissue samples. Representative IHC images and quantitative analysis results in our HCC cohort are shown in Fig. 1C, demonstrating significantly lower STEAP4 expression in HCC tissues compared to adjacent normal tissues ($p < 0.0001$). As presented in Table 1, *STEAP4* expression was not significantly associated with other clinicopathological factors, including lymph node metastasis ($p = 0.212$) and distant metastasis ($p = 0.079$). However, *STEAP4* expression was significantly correlated with tumor T stage ($p = 0.024$) and race ($p = 0.012$) in LIHC patients, suggesting a potential biological role for *STEAP4* in HCC tumor stage progression.

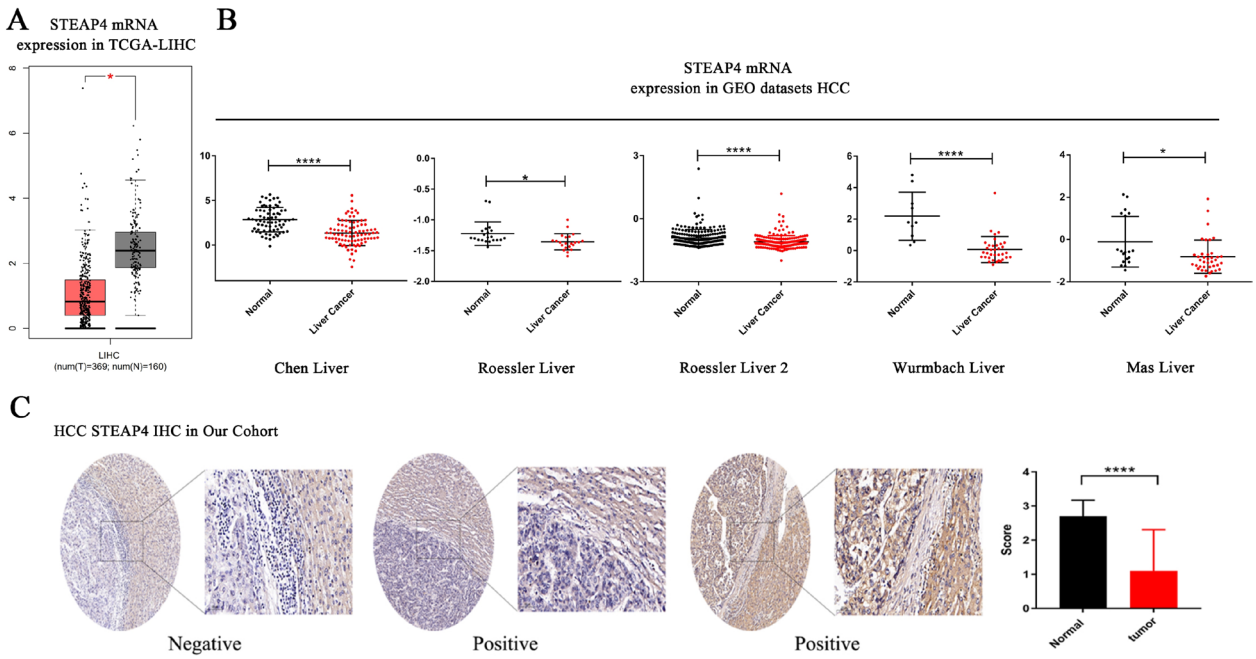

Fig. 1 STEAP4 expression in HCC cohorts. **A** Box plots showing *STEAP4* mRNA expression in liver hepatocellular carcinoma (LIHC) tumor cohort versus TCGA normal and GTEx data, analyzed by t-test in the GEPIA database (*, $p < 0.01$). **B** Scatter plots of *STEAP4* mRNA expression in tumor and non-tumor samples from HCC patients, as presented in the Oncomine database across multiple datasets, including Chen Liver, Roessler Liver, Roessler Liver 2, Wurmbach Liver, and Mas Liver (*, $p < 0.05$; ****, $p < 0.0001$). **C** Representative IHC images (10X and 40X) illustrating STEAP4 protein expression in HCC and adjacent non-tumor tissue. Scale bar = 50 μm for 40X images. Overall statistical analysis of STEAP4 protein expression in HCC patient samples based on IHC staining (****, $p < 0.0001$)

STEAP4 expression is associated with survival in TCGA-LIHC cohort

Patients with higher *STEAP4* expression demonstrated significantly improved overall survival (OS) (log-rank test, $p = 0.024$) and disease-free survival (DFS) (log-rank test, $p = 0.02$), compared to those with lower expression levels in the TCGA-LIHC cohort (Fig. 2A, B). Consistent findings were observed using Kaplan–Meier plotter database with TCGA-LIHC data (Fig. 2C). Multivariate Cox survival analysis further indicated that *STEAP4* expression is an independent predictor of poor prognosis in LIHC patients ($p < 0.05$; Fig. 2D). These results suggest that *STEAP4* may serve as a valuable and independent prognostic marker in HCC.

Genome-wide expression profiles and co-expression networks of *STEAP4* reveal correlations with major cell cycle-regulating genes in TCGA-LIHC cohort

We identified differentially expressed genes (DEGs) by comparing high- and low-expression groups of the *STEAP4* gene within the TCGA-LIHC cohort. In total, 142 upregulated and 250 downregulated genes were significantly associated with *STEAP4* expression (FDR-adjusted $P < 0.05$, FDR < 0.05, and $|FC| \geq 2$, Fig. 3A). As shown in Fig. 3B, the downregulated gene set was significantly enriched for the cell cycle pathway in KEGG analysis. We further examined correlations between *STEAP4* and key cell cycle-related genes (Fig. 3C and Table 2). Results indicated that *STEAP4* expression was significantly correlated with 14 cell cycle-related genes, with the top five negatively regulated genes being *CDC20*, *CDC25C*, *CCNB1*, *CCNB2*, and *PLK1* (all p-values < 0.05, correlation coefficients -0.45, -0.41, -0.41, -0.40, and -0.38, respectively). Notably, IHC staining of our HCC samples revealed significantly higher expression of PLK1, CDC20, CDC25C, and CDK1 in HCC tissues compared to adjacent normal tissues, consistent with the mRNA expression profiles observed in the TCGA-LIHC dataset (Fig. 4).

For further validation, *STEAP4* co-expression genes were analyzed using the LinkedOmics database. Interestingly, differential expression analysis of the top 10 co-expressed genes revealed that 7 of these (*CDT1, CDCA3, KIF2C, BIRC5, TROAP, AURKB,* and *MYBL2*) were closely related to cell cycle regulation. Moreover, *STEAP4* expression in HCC showed significant association with a network of kinases (*ATR, CDK1, CDK2, ATM, PLK1, CHEK1, AURKB,* and *CHEK2*) involved in cell cycle regulation, suggesting a potential role for *STEAP4* in modulating the cell cycle in HCC.

Table 1 Association of *STEAP4* expression with clinicopathological characteristics in TCGA-liver hepatocellular carcinoma (LIHC) patients

Factors	n = 371	High groups (n = 186)	Low groups (n = 185)	*P**
Gender				
Male	250	131	119	0.210
Female	121	55	66	
Ages(years)				
21–40	34	17	17	0.931
41–60	143	72	71	
61–80	183	93	90	
81–100	10	4	6	
NA	1			
Tumor Stage				
T1	181	103	78	**0.024**
T2	94	41	53	
T3	80	32	48	
T4	13	7	6	
TX	1	1	0	
NA	2			
Lymph Node Stage				
N0	252	121	131	0.212
N1	4	1	3	
Nx	114	64	50	
Meteastasis Stage				
M0	266	124	142	0.079
M1	4	3	1	
Mx	101	59	42	
Race Category				
White	183	107	76	**0.012**
Asian	158	64	94	
Other	20	10	10	
NA	10	5	5	
BMI				
<18.5	21	7	14	0.133
18.5–24.9	156	76	80	
25–29.9	90	43	47	
30–34.9	37	19	18	
35–39.9	20	15	5	
≥40	11	7	4	
NA	36	19	17	

*P Chi—square test

Significance in bold, $p < 0.05$.

Effect of *STEAP4* copper reductase activity on HCC cell viability, clonogenicity, and proliferation

To investigate the role of STEAP4 expression in the cell cycle of HCC cell line, we first examined whether STEAP4 overexpression affects viability in the Hep G2 cell line, where baseline STEAP4 expression is low, as shown in the Human Protein Atlas from liver cancer cell lines (Fig. S1). Our western blot results indicated that successfully overexpress or downregulate STEAP4 protein in Hep G2 cells (Fig. S1). Unexpectedly, STEAP4 overexpression did not significantly alter cell viability (Fig. 5A). Given that STEAP4 functions in copper reductase activity involved in copper metabolism [32] and that regulating copper homeostasis can induce programmed cell death [33], we tested the combined effect of STEAP4 overexpression and copper treatment. Treatment with $CuSO_4$ or $CuCl_2$ at high concentrations (over 100 μM) increased cell death in Hep G2 cells (Fig. 5B). However, at low concentrations (25 or 50 μM), both copper compounds promoted cell proliferation (Fig. 5C). We therefore used 50 μM copper as a non-cytotoxic concentration for further analysis.

Interestingly, the combination of STEAP4 overexpression and 50 μM copper significantly reduced cell viability compared to copper treatment alone (Fig. 5D). Rescue experiments using *STEAP4*-targeting siRNA confirmed that STEAP4 is required to enhance cell death under low-copper conditions in Hep G2 cells (Fig. 5D). These findings were corroborated by colony formation assays, which demonstrated that STEAP4 overexpression in combination with 50 μM copper reduced colony formation than copper alone (Fig. 5E, F).

Importantly, results demonstrate that 50 μM copper significantly increases EdU + Hep G2 cells (green) alone (Fig. 6A, B). Conversely, co-treatment with 50 μM copper and STEAP4 overexpression significantly decreases EdU + cells (Fig. 6A, B), a synergistic effect abolished by *STEAP4* knockdown via siRNA. Collectively, STEAP4 with copper reductase activity (at the non-cytotoxic 50 μM concentration) reduces cell viability, clonogenicity, and proliferation in Hep G2 cells.

Effects of STEAP4 and copper reductase activity on cell cycle regulation and cell cycle-related gene expression in HCC

To examine the synergistic effect of STEAP4 with copper reductase activity on cell cycle regulation (Figs. 3B, 6C), we conducted PI staining to assess whether co-treatment with 50 μM copper and STEAP4 overexpression would induce cell cycle arrest in Hep G2 cells. Flow cytometry results indicate that STEAP4 overexpression significantly increases the percentage of Hep G2 cells in sub-G1 and G2/M phases (Fig. 7A–C) when co-treated with 50 μM copper, an effect eliminated by STEAP4 knockdown with

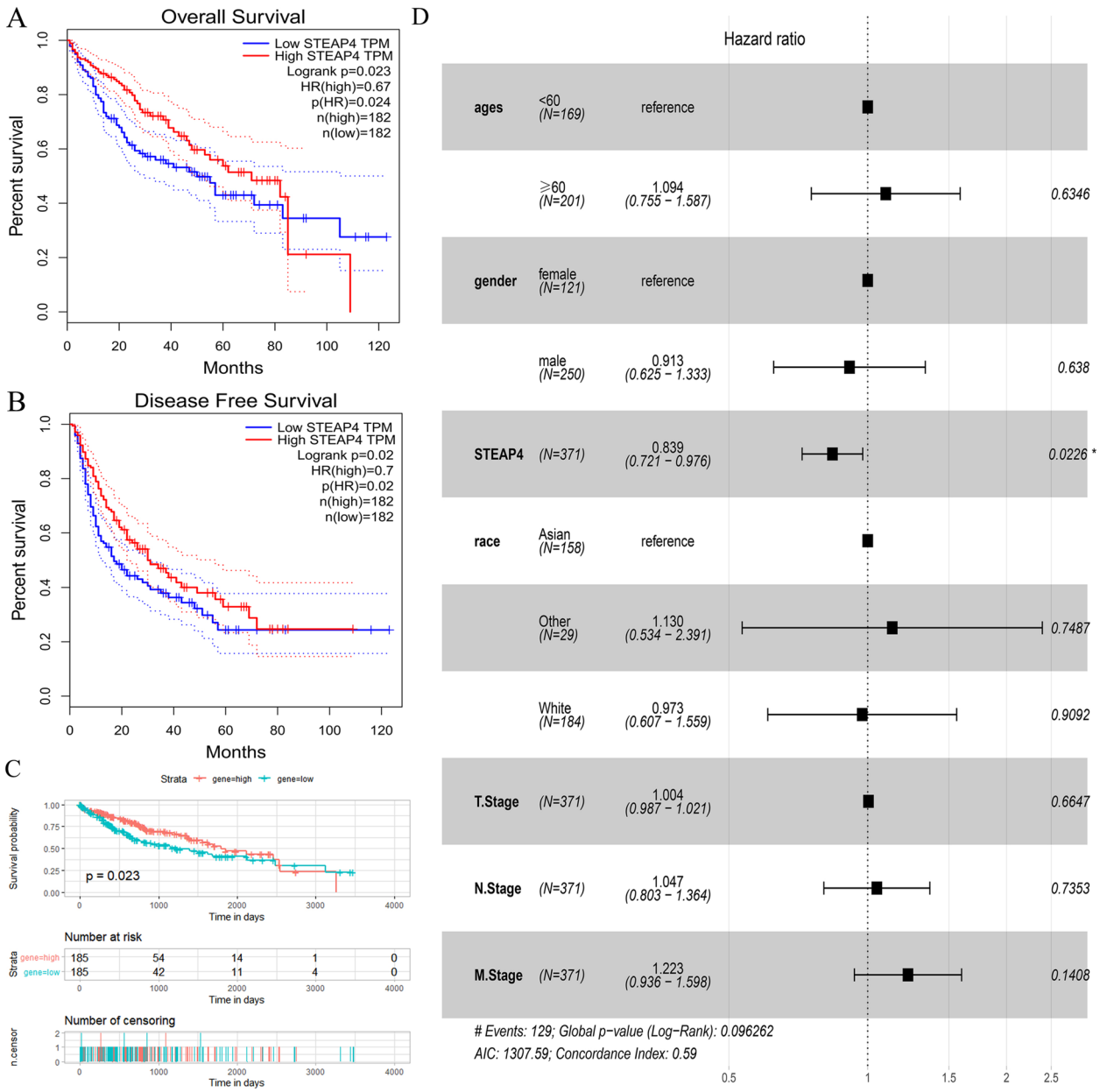

Fig. 2 Prognostic evaluation of *STEAP4* in HCC patients. **A**, **B** Analysis of overall survival (OS) and disease-free survival (DFS) based on high and low *STEAP4* expression in LIHC patients using the GEPIA database. **C** Kaplan–Meier analysis of OS for high and low *STEAP4* expression in TCGA-LIHC samples. **D** Multivariate Cox proportional hazards analysis of OS, visualized through a forest plot

siRNA, suggesting G2/M arrest is linked to STEAP4 with copper reductase activity.

Consistently, co-treatment with STEAP4 overexpression and 50 µM copper significantly downregulates *PLK1, CDK, CDC20, CDC25C, and CCNB2* mRNA expression in Hep G2 cells ($P < 0.05$, respectively, Fig. 8A). Notably, this co-treatment also significantly reduced the protein expression levels of PLK1, CDK, CDC20, CDC25C, and CCNB2 in Hep G2 cells (Fig. 8B). Thus, STEAP4 with copper reductase activity (50 µM as a non-cytotoxic concentration) may induce G2/M phase arrest in HCC cells.

Development and validation of a prognostic model based on *STEAP4*/cell cycle-related genes in HCC

For clinical applicability, we combined seven co-expressed cell cycle genes (*CDT1, CDCA3, KIF2C, BIRC5, TROAP, AURKB, MYBL2*), eight co-expressed cell cycle-related kinases (*ATR, CDK1, CDK2, ATM, PLK1,*

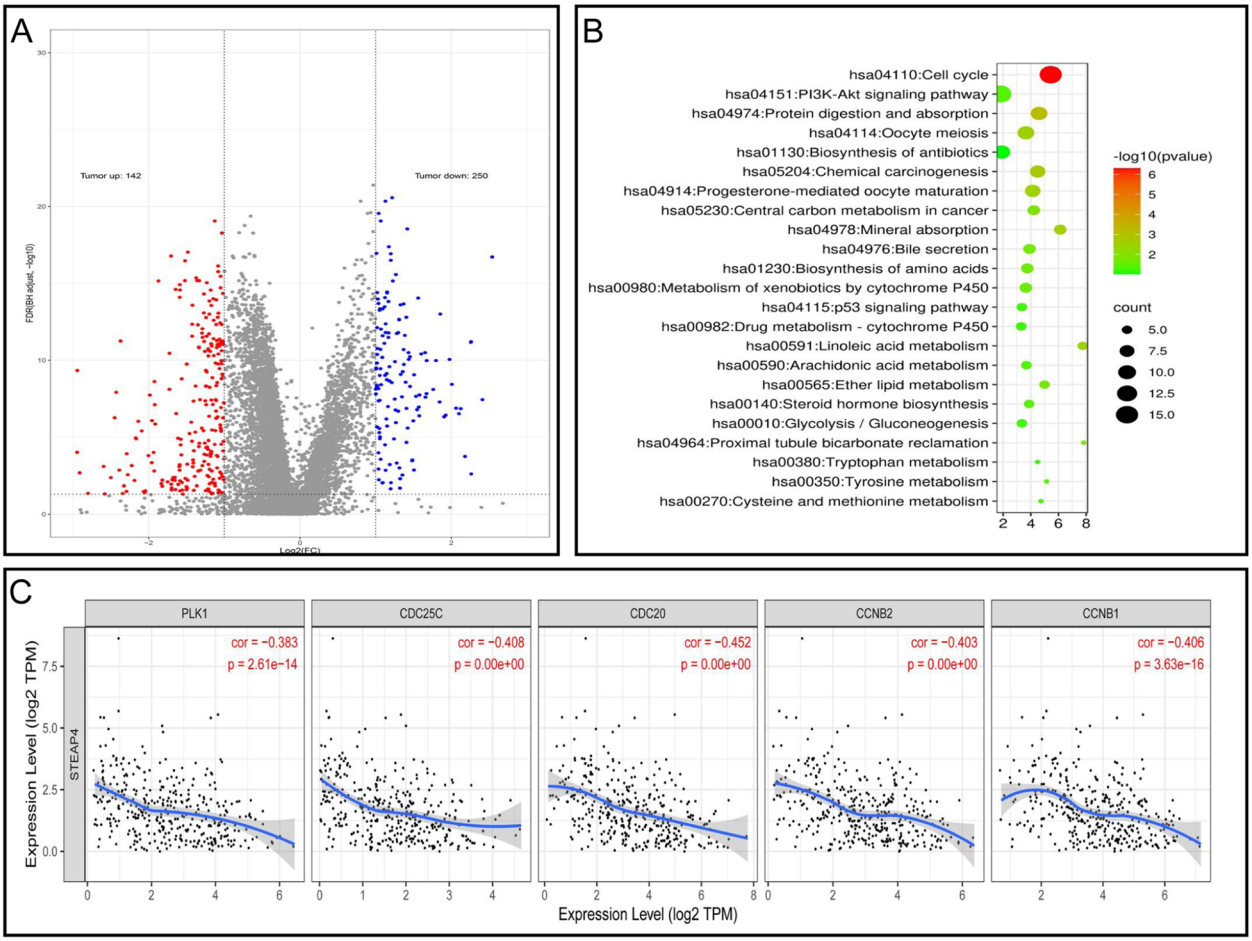

Fig. 3 DEGs of key cell cycle-related genes in high and low *STEAP4* expression groups in LIHC cohort. **A** Volcano plots display differentially expressed genes (DEGs)**. B** KEGG pathway enrichment analysis of DEGs, conducted using DAVID, is visualized in bubble plots, with the y-axis showing significantly enriched KEGG pathways and the x-axis showing various gene ratios. DEGs, differentially expressed genes; KEGG, Kyoto Encyclopedia of Genes and Genomes. **C** The top 5 negatively correlated cell cycle-related genes with *STEAP4*, analyzed using TIMER

Table 2 The correlation between SEAP4 and key cell cycle-related genes in the LIHC-TCGA cohort

14 co-expressed cell cycle-related genes							
varX	**varY**	**cor**	***p***	**varX**	**varY**	**cor**	***p***
TTK	*STEAP4*	− 0.356172319	*2.13E−12*	*CDC25C*	*STEAP4*	− 0.408453554	*/*
SLC25A15	*STEAP4*	0.4116897	*/*	*CDC25A*	*STEAP4*	− 0.366645909	*4.11E−13*
SFN	*STEAP4*	− 0.216287941	*2.65E−05*	*CDC20*	*STEAP4*	− 0.452171727	*/*
PTHLH	*STEAP4*	− 0.185388953	*0.000330727*	*CCNB2*	*STEAP4*	− 0.403449054	*/*
PLK1	*STEAP4*	− 0.382546994	*2.61E−14*	*CCNB1*	*STEAP4*	− 0.406134508	*3.63E−16*
CDK1	*STEAP4*	− 0.368527766	*3.03E−13*	*BUB1B*	*STEAP4*	− 0.322504506	*2.53E−10*
CDC6	*STEAP4*	− 0.3251353	*1.78E−10*	*BUB1*	*STEAP4*	− 0.322642214	*2.49E−10*
CDC45	*STEAP4*	− 0.363113431	*7.24E−13*				

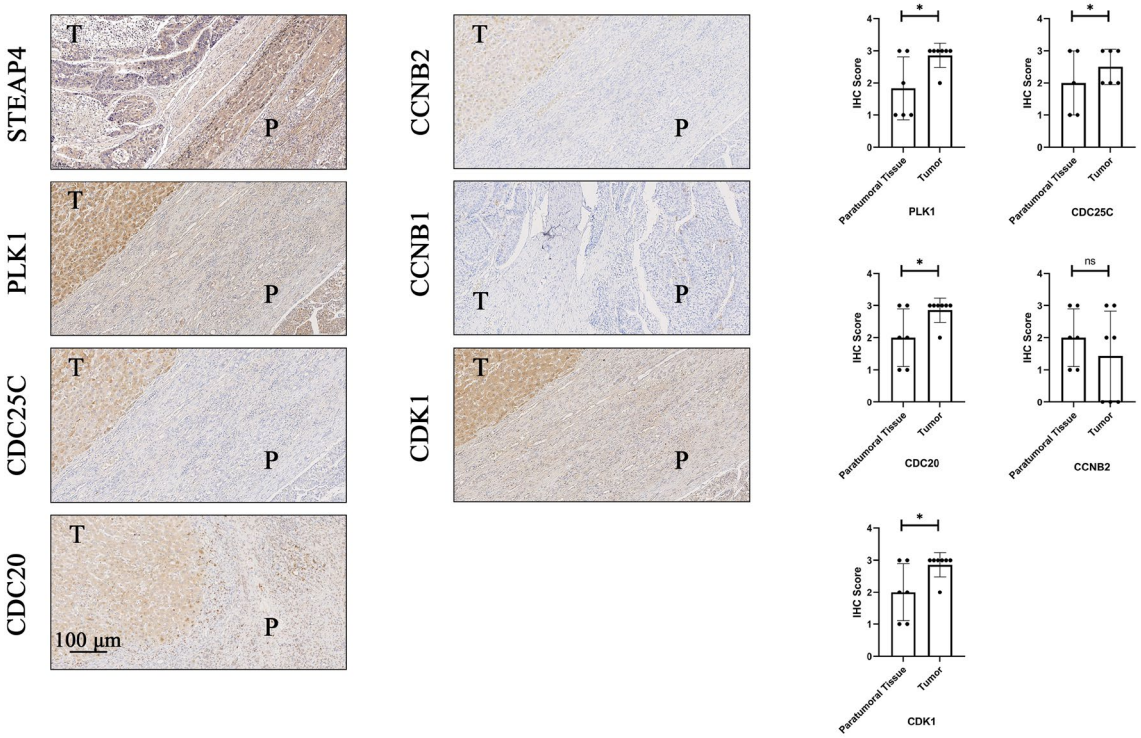

Fig. 4 Representative IHC images showing the expression of STEAP4, PLK1, CDC25C, CDC20, CCNB2, CCNB1, and CDK1 proteins in HCC and adjacent non-tumor tissues. Compared to peritumoral tissues, HCC tissues exhibit lower STEAP4 expression and higher levels of PLK1, CDC20, CDC25C, and CDK1 (n = 7). T: tumor; P: peritumoral tissue. Scale bar: 100 μm

CHEK1, AURKB, CHEK2), and *STEAP4* to develop a prognostic model for HCC. Using multivariate Cox proportional hazards regression and stepwise analysis, we created an optimal model: **risk score = *CDCA3**** **0.5289133 + *STEAP4**** **− 3.7328420**. Patients were classified into high- and low-risk groups based on median risk score. The high-risk group had significantly shorter OS (***P* **< 0.0001,** Fig. 9A), with AUCs of 0.783, 0.722, and 0.754 for 1-, 3-, and 5-year OS, respectively (Fig. 9C). The risk score was validated as an independent prognostic factor through multivariate analysis (Fig. 9D). Subgroup analysis further validated the signature's prognostic value across stages, sexes, and age groups (Fig. 9E)**.** The signature model ability stratifying patients was achieved in patients with early-stage, advanced stage, male, female, < 60-year, < 60-year, and > = 60-year, respectively.

The predictive capability of this signature was validated in the ICGC dataset. Patients were stratified into high- and low-risk groups using the same method. Survival analysis showed lower OS in high-risk patients ($p = 0.0088$) (Fig. 10A). Scatter plots and heat maps depict risk score distribution, patient survival status, and gene expression patterns (Fig. 10B). AUCs were 0.560, 0.684, and 0.951 for 1-, 3-, and 5-year OS, respectively (Fig. 10C). Further validation confirmed the signature as an independent prognostic factor (Fig. 10D). For clinical utility, we combined independent factors from the TCGA cohort to create a nomogram (Fig. 10E). Calibration plots of 1-, 3-, and 5-year survival rates are presented in Fig. 10F.

Discussion

Hepatocellular carcinoma (HCC) constitutes approximately 90% of primary liver tumors and ranks as the second leading cause of cancer-related mortality globally [1] with an overall poor survival rate [34]. Despite its prevalence, the molecular pathogenesis of HCC remains incompletely understood [2]. In this study, we demonstrate that *STEAP4* expression is significantly reduced in the TCGA-LICH cohort, and low *STEAP4* expression is associated with worse prognosis and overall survival in HCC patients. Functional network analysis indicated that *STEAP4* is involved in cell cycle regulation. Overexpression of STEAP4, combined with exposure to a non-cytotoxic concentration of copper in HepG2 cells, reduced proliferation and clonogenicity, induced cell cycle arrest, and downregulated mRNA expression and protein expression of indicated cell cycle-related genes. The prognostic relevance of STEAP4's copper reductase activity in HCC suppression, along with its associations

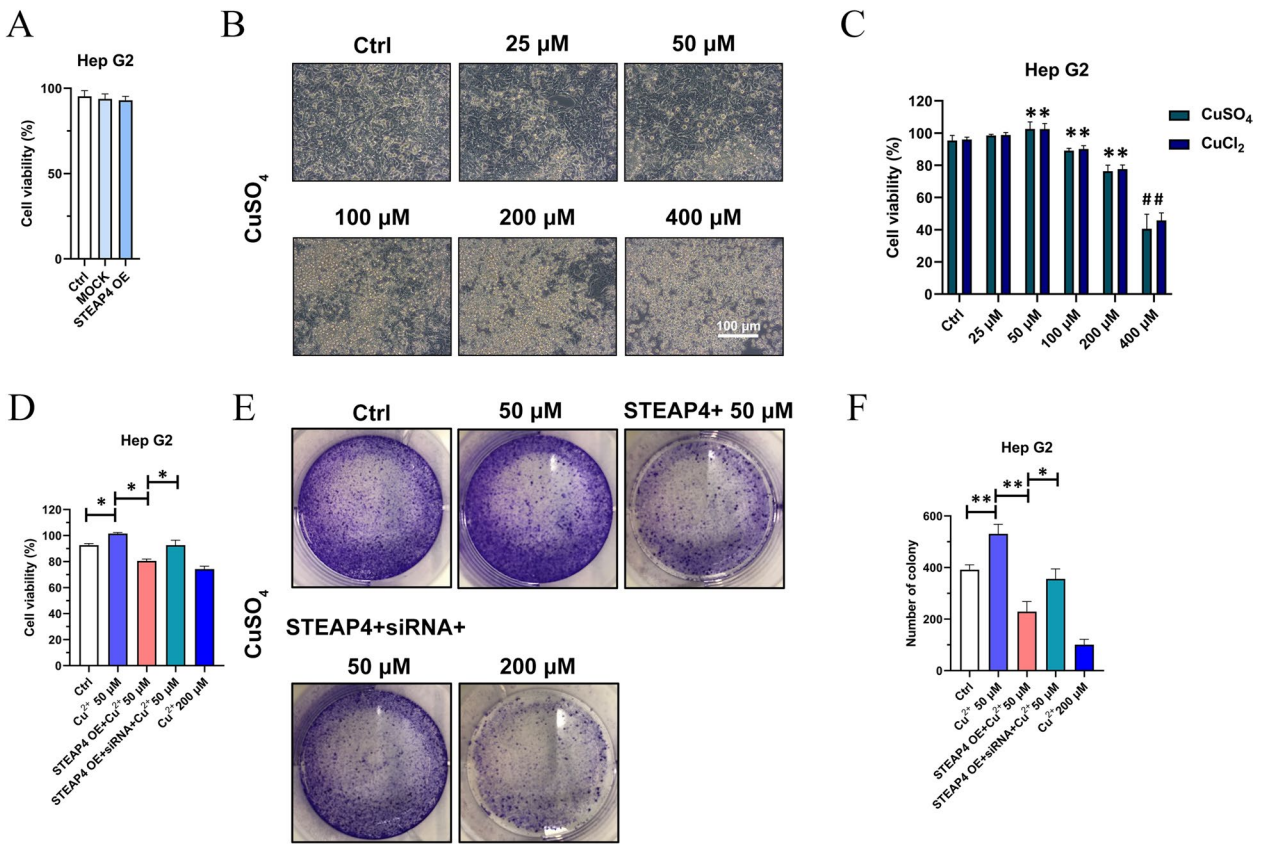

Fig. 5 Efficacy of STEAP4 overexpression in Hep G2 Cells via copper reductase activity**. A** STEAP4 overexpression in Hep G2 cells shows no significant cytotoxicity. **B**, **C** Copper incubation induces a dose-dependent cytotoxic effect on Hep G2 cells, with 50 μM copper identified as a non-cytotoxic concentration. **D** Co-treatment with STEAP4 overexpression and 50 μM copper decreases cell viability in Hep G2 cells. **E**, **F** Co-treatment with STEAP4 overexpression and 50 μM copper reduces colony formation in Hep G2 cells. *$p < 0.05$, **$p < 0.01$, ***$p < 0.001$, ##$p < 0.0001$

with cell cycle control kinases, may provide promising insights for future therapeutic targets (Fig. 11).

The STEAP gene family, initially identified in 1999 by Hubert et al. in a prostate cancer xenograft model [9], includes *STEAP4*, which is expressed in various tissues, such as lung, pancreas, heart, liver, and skeletal muscle [5–8]. Studies have shown that *STEAP4* downregulation contributes to inflammation [35, 36], and is implicated in prostate [8, 37], colon [15, 38], breast [17, 39] and bladder cancer progression [19]. However, the role of STEAP4 in HCC remains largely unexplored [2, 18]. To investigate, we used bioinformatics to analyze *STEAP4*'s function and regulatory network in HCC, revealing significant downregulation in HCC cohorts and a correlation with poorer prognosis and survival in the TCGA-LIHC dataset, suggesting a tumor-suppressive function. Subgroup analysis showed that *STEAP4* levels correlate with T stage, making it a potential diagnostic and prognostic marker. High *STEAP4* expression was associated with an increased proportion of T1 stage cases. Multivariate Cox analysis confirmed *STEAP4* as an independent predictor of unfavorable prognosis in LIHC patients ($p < 0.05$).

Through the LinkedOmics database, we identified 9,839 co-expressed genes, with KEGG pathway analysis showing enrichment in pathways like Complement and coagulation cascades, Chemical carcinogenesis, Fatty acid degradation, Spliceosome, Ribosome, and Cell cycle. *STEAP4* was notably correlated with 14 cell cycle genes, including *CDC20, CDC25C, CCNB1, CCNB2, and PLK1*, as well as kinases like *ATR, CDK1, CDK2, ATM, PLK1, CHEK1, AURKB, and CHEK2*, which regulate DNA damage, replication, mitosis, and cell cycle control. Elevated expression of cancer-related kinases (*AURKB, CDK1, CHEK1, and PLK1*) correlated with poor HCC prognosis. PLK1, which controls the G2/M phase, was highly expressed in multiple cancers [40], with aberrant PLK1-related pathway activation in HCC [41, 42]. Longerich's study showed that PLK1 plays oncogenic role in HCC [43]. Additionally, ATR-CHEK1 signaling, crucial for DNA damage response and genomic stability [44, 45], has

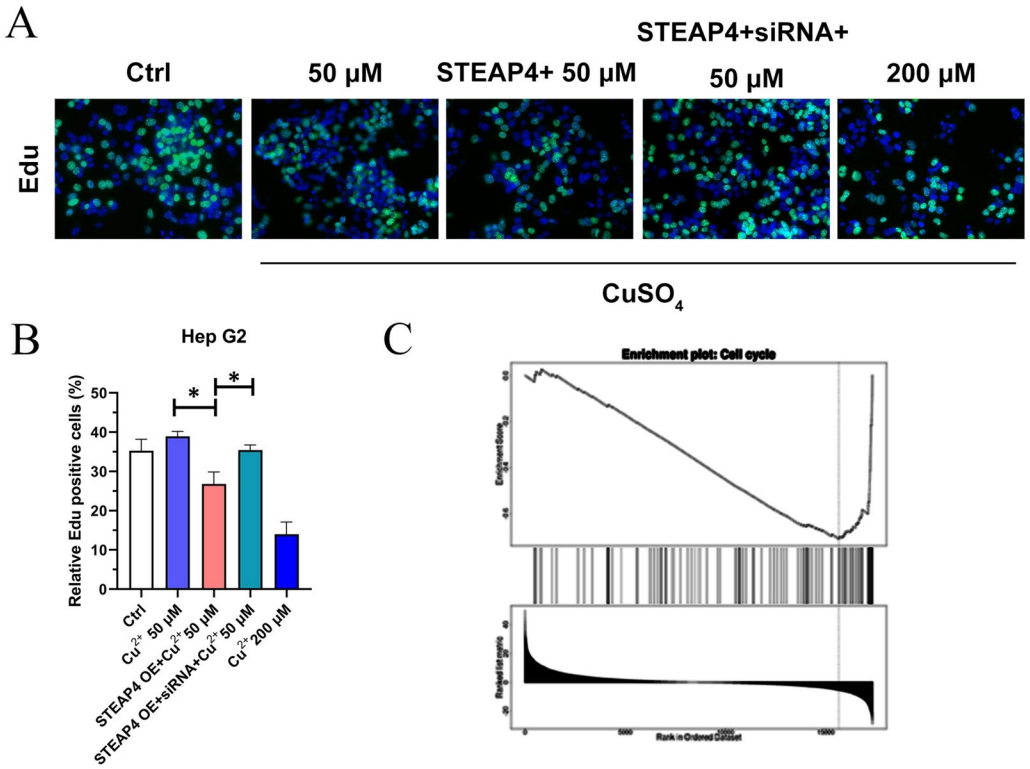

Fig. 6 Inhibition of Hep G2 cell proliferation by STEAP4 with copper reductase activity. **A**, **B** The 5-Ethynyl-2′-deoxyuridine (EdU) staining reveals reduced cell proliferation rates following STEAP4 overexpression with 50 μM copper co-treatment. **C** GSEA of the LICH-TCGA cohort highlights *STEAP4* co-expressed genes linked to cell cycle regulation. * $p < 0.05$

been linked to HCC progression [46, 47]. AURKA overexpression promotes HCC proliferation and metastasis, suggesting the need for further research on STEAP4's interaction with these kinases. However, further research on the association mechanism between STEAP4 and these cell cycle control kinases is needed.

The study reveals that STEAP4 plays a crucial role in modulating copper homeostasis, which appears directly linked to its tumor-suppressive effects in HCC. STEAP4's copper reductase activity facilitates intracellular copper reduction, a process that impacts key cell cycle regulators and cancer progression. By promoting copper reduction, STEAP4 appears to influence cell cycle checkpoints, particularly in the G2/M phase. STEAP4-mediated copper reduction has been shown to induce G2/M phase arrest, indicating a novel mechanism whereby STEAP4 hinders cell proliferation by modulating copper availability. Furthermore, our data suggests that STEAP4 works in synergy with copper at non-cytotoxic levels to inhibit HCC cell viability, colony formation, and proliferation. The combined effect of STEAP4 expression and controlled copper levels disrupts cellular processes critical for cancer progression. This interplay highlights STEAP4's potential as a regulatory mediator between copper metabolism and cell cycle control in HCC. Notably, recent studies have shown that copper acts as a co-factor in multiple oncogenic pathways, yet its dysregulation is also linked to oxidative stress and apoptosis in tumor cells. Thus, STEAP4's role in fine-tuning copper levels provides a unique checkpoint that may prevent cancerous cells from acquiring an uncontrolled growth advantage. This association not only deepens our understanding of copper's role in oncogenesis but also opens potential avenues for targeting copper metabolism in HCC with altered STEAP4 expression.

Copper impacts cell cycle regulation, interacting with cell cycle proteins at multiple checkpoints. High copper levels influence cyclin-dependent kinase activity, impacting G1/S and G2/M transitions. In our study, STEAP4 overexpression combined with 50 μM copper reduced viability, clonogenicity, proliferation, and induced G2/M arrest in HepG2 cells. The synergy effect was abolished by STEAP4 knockdown, indicating that G2/M arrest is mediated by STEAP4's copper reductase activity. More importantly, STEAP4-mediated increases in colon cancer copper levels result in activation of the E3 ligase X-linked inhibitor of apoptosis (XIAP) [15], cooperation with CDK1–cyclin-B1 axis controlling mitotic cell death [48],

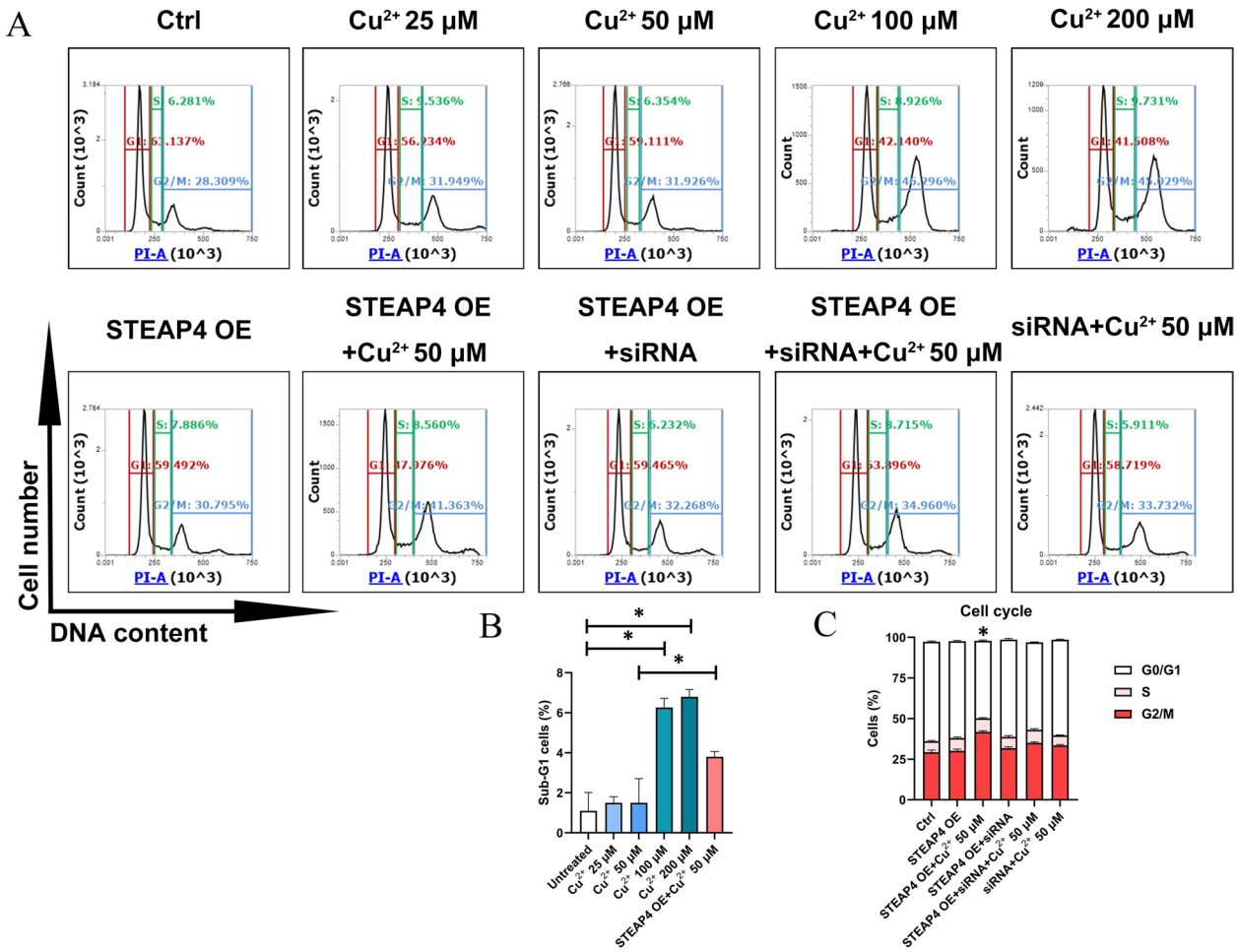

Fig. 7 Effects of *STEAP4* overexpression and 50 μM copper on cell cycle distribution in Hep G2 cells. **A**–**C** Cell cycle distribution analysis shows that co-treatment with STEAP4 overexpression and 50 μM copper increases the percentage of Hep G2 cells in sub-G1 and G2/M phases. The synergistic effect is eliminated by STEAP4 knockdown via siRNA, indicating G2/M cell cycle arrest associated with STEAP4 copper reductase activity. * $p < 0.05$

indicating an important regulatory role of STEAP4 in the cell cycle of malignant tumors [49]. Co-expression of XIAP and Cyclin D1 correlates with HCC outcomes [50], underscoring the role of STEAP4 in malignant cell cycle regulation and copper homeostasis. However, further study is needed for understanding from modulating key cell cycle regulators to orchestrating copper homeostasis through STEAP4.

To advance risk assessment in HCC, we developed a gene expression signature associated with *STEAP4* and co-regulated genes. The two-gene signature (*STEAP4* and *CDCA3*, Figs. 9and10) was successfully constructed via TCGA cohort, and was validated in ICGC cohort, demonstrating robust prognostic power in subgroup analysis. To offer an easy-to-use clinical assay, we also combined this signature with TNM staging to construct a nomogram with high discriminatory accuracy, improving prognostic stratification for resectable HCC patients and aiding in adjuvant treatment selection.

This study has several limitations. First, we did not investigate the cell cycle regulatory function of STEAP4 using in vivo animal models. However, datasets from TCGA suggest a potentially significant role for *STEAP4* in the HCC cohort. Second, the mechanism by which copper supports the cell cycle regulatory function of STEAP4 was not explored. Finally, while our results indicate G2/M phase arrest, the discrepancy between the downregulation of multiple cell cycle proteins and the exclusive observation of G2/M phase arrest warrants further investigation to uncover the underlying mechanisms.

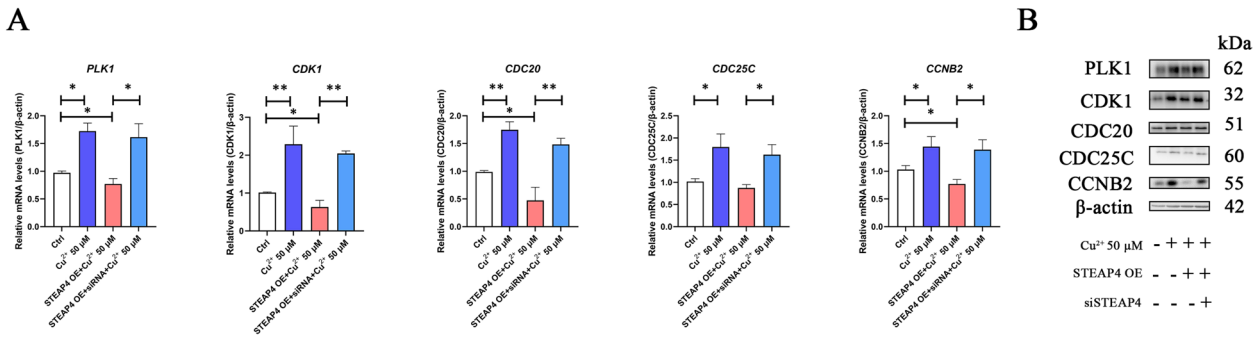

Fig. 8 STEAP4 and 50 μM Copper co-treatment downregulates indicated cell cycle genes in Hep G2 cells. **A** STEAP4 with copper reductase activity reduces *PLK1, CDK1, CDC20, CDC25C, and CCNB2* mRNA expression in Hep G2 cells. This synergistic effect is abolished by *STEAP4* knockdown via siRNA. * $p < 0.05$, ** $p < 0.01$. **B** STEAP4 with copper reductase activity reduces PLK1, CDK1, CDC20, CDC25C, and CCNB2 protein expression in Hep G2 cells as indicated by representative western blot results

Conclusion

Our study provides potential evidence that STEAP4 may play a role in regulating HCC tumorigenesis, underscoring its significance in cell cycle regulation. STEAP4-mediated cell cycle regulation appears to depend on non-cytotoxic copper as a synergistic factor in vitro, supported by its copper reductase activity. These findings may offer new development of therapeutic targets in HCC.

Material and methods

Differential expression analysis of *STEAP4* mRNA and immunohistochemistry (IHC) in cancer samples

The GEPIA database (http://gepia.cancer-pku.cn) and Oncomine 4.5 (https://www.oncomine.org/) were utilized to determine *STEAP4* gene expression levels in normal tissues and hepatocellular carcinoma (HCC) tumors. For subgroup analysis, publicly available liver hepatocellular carcinoma (LIHC) RNA-Seq data were downloaded from The Cancer Genome Atlas (TCGA) database (https://cancergenome.nih.gov/) using the GDC Data Transfer Tool. A total of 371 primary tumor samples were categorized into low (n = 185) and high (n = 186) *STEAP4* expression groups based on the median *STEAP4* mRNA level. Associations between *STEAP4* mRNA expression and clinicopathological features were assessed using the chi-squared test.

All sample section staining procedures were approved by the Ethics Review Board of Third Affiliated Hospital of Sun Yat-sen University under ethics approval number II 2024–196. Immunohistochemical staining was performed as previously described [15]. Briefly, tissue antigens were retrieved using sodium citrate for 15 min, followed by blocking with 5% BSA for 30 min. The tissue section was then incubated overnight at 4 °C with an anti-*STEAP4* antibody (A17767, 1:100, Abclonal, Germany), anti-CDC20 antibody (A15656, 1:100, Abclonal, Germany), anti-CDK1 antibody (A22347, 1:100, Abclonal, Germany), anti-Cyclin B2 antibody (DF9047, 1:100, Affinity Biosciences, USA), anti-PLK1 antibody (AF2685, 1:100, Affinity Biosciences, USA), and anti-CDC25C antibody (AF6258, 1:100, Affinity Biosciences, USA). On the second day, an HRP-conjugated secondary antibody was applied for 120 min, followed by nuclear staining with hematoxylin. Digital images of the stained sections were captured using a Leica DM300 microscope (Germany). The subgroup analysis was performed on frozen primary and recurrent HCC tissue samples, categorizing them based on STEAP4 expression into high and low groups. Staining intensity was classified as 0 for negative, 1 for light yellow, 2 for light brown, and 3 for dark brown. Positive intensity and percentage were recorded, with scores of 0–1 deemed negative and scores of 2–3 deemed positive.

Association analysis between *STEAP4* expression and prognosis

Survival curves, including overall survival (OS) and recurrence-free survival (RFS), were generated through the GEPIA database using the log-rank and Mantel-Cox tests. Survival analysis was conducted with the survival and survminer packages in R version 4.0.5, and independent prognostic factors were identified via multivariate Cox regression.

LinkedOmics database and genome-wide *STEAP4* co-expression analysis

STEAP4 co-expression was analyzed in the LinkedOmics database (http://www.linkedomics.org/login.php) using

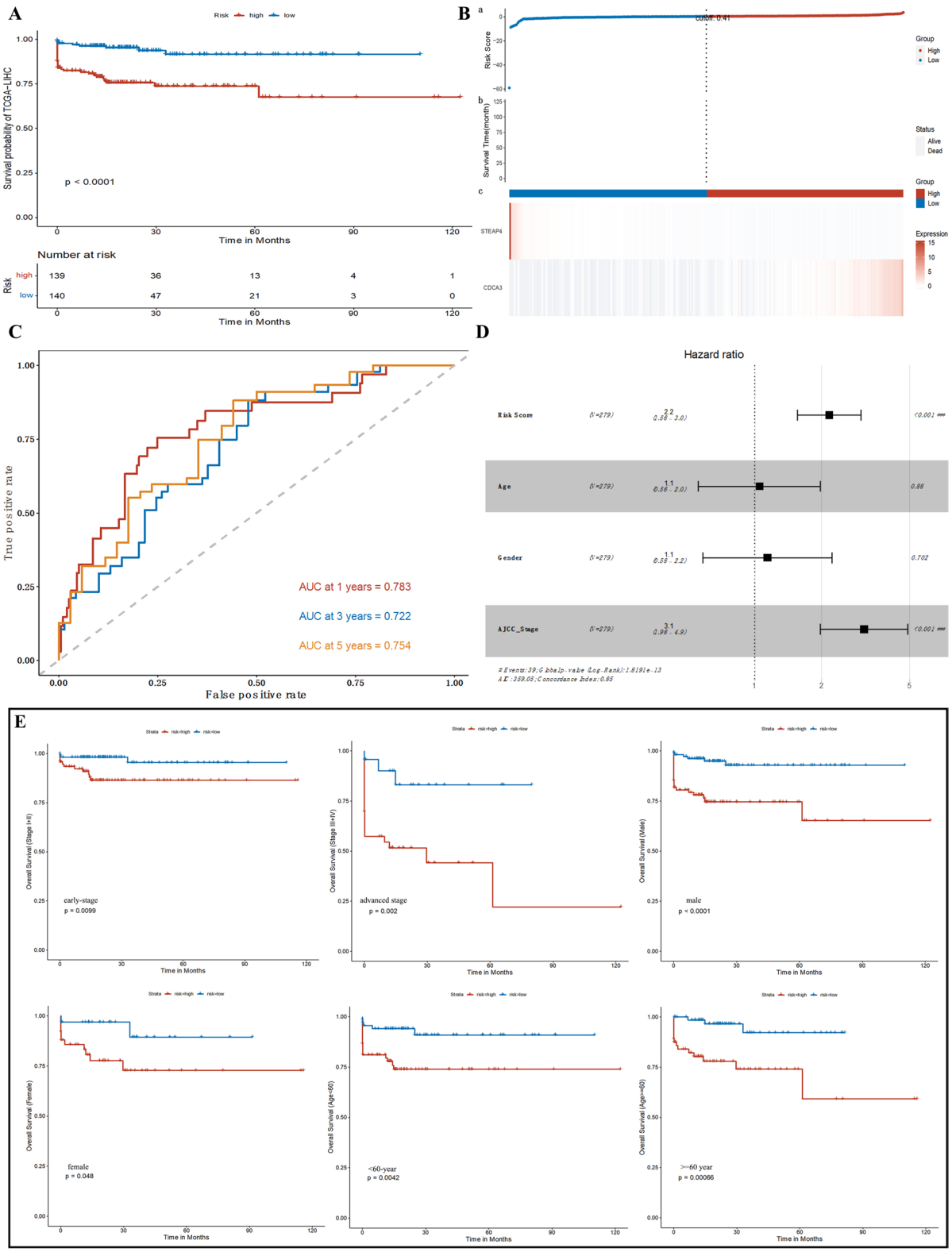

Fig. 9 Prognostic model construction and subgroup analysis. **A** Kaplan–Meier curves and log-rank test show OS differences in high- vs. low-risk groups (TCGA-LIHC). **B** Scatter plots showing gene distribution in the signature. **C** ROC curves evaluating the signature's predictive performance in TCGA-LIHC. **D** Identification of signature as an independent prognostic factor. **E** Subgroup analysis across different clinical factors: early-stage, advanced stage, male, female, < 60-year and ≥60 years, respectively

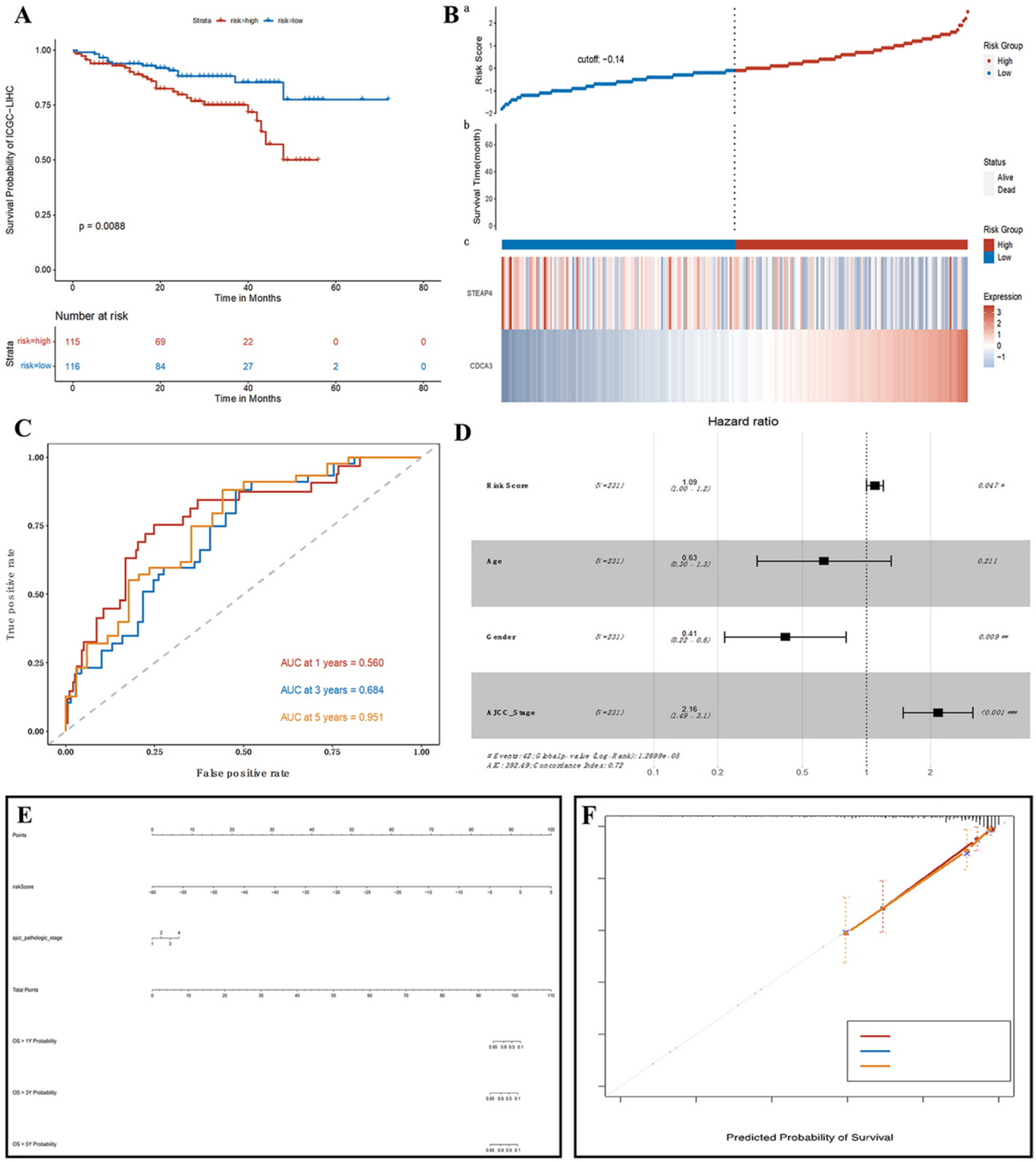

Fig. 10 Signature validation in ICGC-HCC dataset and nomogram development. **A** Kaplan–Meier curves and log-rank test of OS in high- and low-risk groups (ICGC-HCC). **B** Scatter plots of gene expression in the signature. **C** ROC curves assessing prediction performance (ICGC-HCC). **D** Identification of the signature as an independent prognostic factor. **E** Nomogram integrating TNM stage and signature. **F** Calibration plots for survival rates at 1, 3, and 5 years

Pearson's correlation coefficient and presented in volcano plots, heat maps, and scatter plots. LinkedOmics' function module was employed to examine Gene Ontology biological processes (GO_BP), KEGG pathways, and kinase-target enrichment through gene set enrichment analysis (GSEA). Differentially expressed genes among

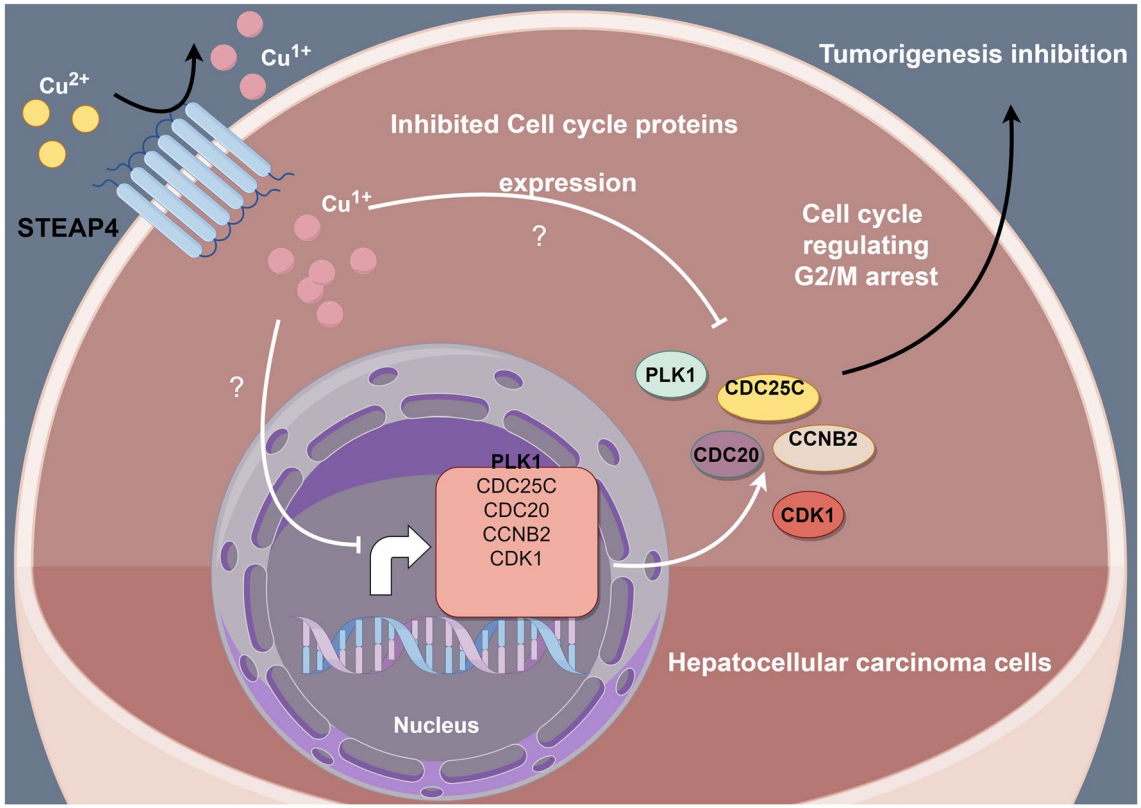

Fig. 11 Schematic diagram of proposed mechanism of STEAP4-mediated copper reductase activity in HCC tumorigenesis suppression via cell cycle regulation. This schematic illustrates STEAP4's functional impact on HCC cells in vitro. STEAP4-mediated copper reduction leads to downregulation of key cell cycle genes, inhibiting G2/M progression in HCC cells. Further investigation into the underlying mechanisms of STEAP4-mediated regulation of cell cycle genes is warranted. (Figure created with Figdraw)

LIHC patients were further verified with the TIME database for *STEAP4* correlation.

Cell Culture and Copper Treatment Conditions

Hep G2 cells (American Type Culture Collection, ATCC, Manassas, MD, USA) were cultured in RPMI 1640 medium with 10% FBS, 1% penicillin, and streptomycin at 37 °C with 5% CO_2. $CuSO_4$ and $CuCl_2$ (Cayman Chemical) were dissolved in ddH_2O and adjusted to the required concentration. Cells were treated with copper for 48 h post-STEAP4 overexpression or knockdown unless otherwise specified.

STEAP4 overexpression and knockdown via transient transfection

Approximately 1×10^5 cells/well were seeded in 6-well plates at 50–70% confluence. *STEAP4* overexpression or knockdown was achieved with Lipofectamine® 3000 Reagent following the manufacturer's protocol. Transfection involved pCMV6-Entry-*STEAP4* (NM_024636) Human ORF Clone plasmid (500 ng, RC216917, Origene) for overexpression or 10 nmol of STAMP2 siRNA (Santa Cruz, Germany) for knockdown. Empty vector or control siRNA served as MOCK or knockdown control. STEAP4 protein expression was used to confirm transfection efficiency.

Cell viability assay

Cell viability was assessed by crystal violet staining as described previously [31]. Approximately 1×10^4 cells/well were seeded in 12-well plates, treated with copper (with or without *STEAP4* overexpression) for 48 h, washed with PBS, and stained with 0.1% crystal violet for 30 min. Absorbance was measured at 595 nm using a microplate reader (Tecan, Germany). Cell morphology post-treatment was examined using phase-contrast microscopy (Carl Zeiss, Germany).

Colony formation assay

The colony formation assay was conducted as previously described. Briefly, 200 single cells were seeded per well in

Table 3 The qRT-PCR primers used in this study (Homo sapiens)

Genes	Forward	Reverse
PLK1	AAAGAGATCCCGGAGGTCCTA	GGCTGCGGTGAATGGATATTTC
CDK1	AAACTACAGGTCAAGTGG TAGCC	TCCTGCATAAGCACATCCTGA
CDC20	GCACAGTTCGCGTTCGAGA	CTGGATTTGCCAGGAGTTCGG
CDC25C	TCTACGGAACTCTTCTCA TCCAC	TCCAGGAGCAGGTTTAAC ATTTT
CCNB2	CCGACGGTGTCCAGTGATTT	TGTTGTTTTGGTGGGTTGAACT
β-actin	GCCGCCAGCTCACCA	GCTCGATGGGGTACTTCAGG

6-well plates and cultured for seven days. Colonies were stained with 0.1% crystal violet, and morphology was observed using phase-contrast microscopy (Carl Zeiss, Germany).

The 5-ethynyl-2′-deoxyuridine (EdU) staining for DNA synthesis detection

To assess DNA synthesis and cell cycle S-phase, Hep G2 cells were stained using the Click-iT™ EdU Cell Proliferation Kit (Invitrogen, Germany) following the manufacturer's instructions.

Propidium iodide (PI) staining for cell cycle analysis by flow cytometry

Forty-eight hours post-treatment with copper, Hep G2 cells underwent PI/RNase A staining (Invitrogen, Germany) for cell cycle analysis by flow cytometry (BD Accuri C6, Beckman Coulter, Germany), analyzing phases sub-G0/G1, G0/G1, S, and G2/M in over 25,000 cells.

Real-time quantitative PCR (qRT-PCR)

Total RNA was extracted with TRIzol reagent (Invitrogen), and qRT-PCR was performed using SYBR green qPCR master mix (TAKARA, Japan) following the manufacturer's protocol. Primers are listed in Table 3, with β-actin as an internal reference for mRNA normalization. Determine the relative mRNA expression levels of target genes was using the $2^{-\Delta\Delta Ct}$ method.

Western blotting

Cells were harvested and lysed in RIPA buffer, and protein concentrations were quantified using a BCA assay (Invitrogen, Germany). Following SDS-PAGE separation, protein samples were blocked in 5% skim milk and incubated overnight at 4 °C with primary antibodies: anti-STEAP4 antibody (11944-1-AP, 1:2000, proteintech, Germany), anti-PLK1 antibody (10305-1-AP, 1:2000, proteintech, Germany), anti-CDC20 antibody (10252-1-AP, 1:2000, proteintech, Germany), anti-Cyclin B2 antibody (21644-1-AP, 1:2000, proteintech, Germany), anti-CDC25C antibody (16485-1-AP, 1:2000, proteintech, Germany) and anti-CDK1/CDK2 antibody (sc-53219, 1:2000, Santa Cruz, Germany). Samples were then washed five times with TBST and incubated with appropriate secondary antibodies for 2 h at room temperature. Protein bands were visualized with Immobilon Western Chemiluminescent HRP Substrate (Millipore, WBKLS0500) for 1 min, and band densities were normalized to β-actin.

Establishment and validation of the prognostic model

To construct a prognostic model, we integrated co-expression genes and regulators of *STEAP4* and applied stepwise multivariate Cox regression analysis based on the Akaike Information Criterion (AIC) to minimize overfitting and select candidate genes. Each LIHC patient's risk score was calculated using the formula: risk score = gene a * coefficient a + gene b * coefficient b + gene c * coefficient c + … + gene n * coefficient n. Patients were then stratified into high- and low-risk groups based on the median risk score. Kaplan–Meier survival curves compared survival between these groups, and the log-rank test assessed statistical significance ($p < 0.05$). Model performance was evaluated and validated in both the TCGA-LIHC and ICGC-LIHC cohorts. The model visualization was facilitated through a nomogram, and calibration plots assessed prediction accuracy.

Statistical analysis

Statistical analysis was conducted using SPSS 25.0 and R version 4.0.5. Data are presented as mean ± SD. Differential expression of *STEAP4* mRNA between HCC and adjacent normal tissues from the TCGA databases was analyzed via independent and paired t-tests. IHC staining scores were analyzed via Wilcoxon Signed-Rank Test. Associations between *STEAP4* and clinical variables were examined using Pearson's chi-squared test. Multivariate analyses were performed using the Cox proportional hazards model. Statistical significance was set at $P < 0.05$.

Supplementary Information

The online version contains supplementary material available at https://doi.org/10.1186/s13008-024-00140-y.

Supplementary Material 1.

Supplementary Material 2.

Acknowledgements
The schematic diagram figure was drawn by Figdraw (https://www.figdraw.com/static/index.html). We thank the National Key Clinical Specialty (Medical Imaging Department) Construction Project for the support in this study.

Author contributions
T.Y. conceptualized and designed the study, performed in-vitro experiments, performed data analysis, and contributed to manuscript drafting. Mh.Z. analyzed the data and executed the histological examination. Yj.X. analyzed the data. Sh.J. performed in-vitro experiments, contributed to manuscript drafting. Y.Z., Sh.J., and Q.Z.were the major contributors to revising the manuscript. Y.Z., K.W. and Q.Z. supported the study with supervision, project administration, and funding acquisition. All authors participated in manuscript revision, read and approved the final version of the manuscript.

Funding
This research was supported by the National Science Foundation Cultivation Project of Third Affiliated Hospital of Sun Yat-sen University (2021GZRPYQN03). This research was supported by the National Key Clinical Specialty (Medical Imaging Department) Construction Project. This research was partly supported by the Guangzhou Key Research and Development Project (No. 2023B03J0211) and the Science and Technology Planning Project of Guangdong Province (No. 2023A1515012621).

Data availability
The data generated or analyzed in this study are available within the article and its supplementary materials, and available from the corresponding author upon request.

Declarations

Ethics approval and consent to participate
All procedures in this study were conducted in accordance with the Ethics Committee of Third Affiliated Hospital of Sun Yat-sen University. Sample section staining related to this study were conducted in accordance with Declaration of Helsinki, and with the Ethics review board of Third Affiliated Hospital of Sun Yat-sen University with ethics approval number (II 2024-196). Consent was obtained from the participant.

Competing interests
The authors declare no competing interests.

Received: 26 May 2024 Accepted: 13 December 2024
Published online: 24 December 2024

References

1. Singh A, Beechinor RJ, Huynh JC, Li D, Dayyani F, Valerin JB, Hendifar A, Gong J, Cho M. Immunotherapy updates in advanced hepatocellular carcinoma. Cancers (Basel). 2021;13:2164.
2. Yamada N, Yasui K, Dohi O, Gen Y, Tomie A, Kitaichi T, Iwai N, Mitsuyoshi H, Sumida Y, Moriguchi M, Yamaguchi K, Nishikawa T, Umemura A, Naito Y, Tanaka S, Arii S, Itoh Y. Genome-wide DNA methylation analysis in hepatocellular carcinoma. Oncol Rep. 2016;35:2228–36.
3. Liu Y, Yang Y, Luo Y, Wang J, Lu X, Yang Z, Yang J. Prognostic potential of PRPF3 in hepatocellular carcinoma. Aging (Albany NY). 2020;12:912–30.
4. DiStefano JK, Davis B. Diagnostic and prognostic potential of AKR1B10 in human hepatocellular carcinoma. Cancers (Basel). 2019;11:486.
5. Li PL, Liu H, Chen GP, Li L, Shi HJ, Nie HY, Liu Z, Hu YF, Yang J, Zhang P, Zhang XJ, She ZG, Li H, Huang Z, Zhu L. STEAP3 (six-transmembrane epithelial antigen of prostate 3) inhibits pathological cardiac hypertrophy. Hypertension. 2020;76:1219–30.
6. Schober SJ, Thiede M, Gassmann H, Prexler C, Xue B, Schirmer D, Wohlleber D, Stein S, Grunewald TGP, Busch DH, Richter GHS, Burdach SEG, Thiel U. MHC class I-restricted TCR-transgenic CD4(+) T cells against STEAP1 mediate local tumor control of ewing sarcoma in vivo. Cells. 2020;9:1581.
7. Yang Q, Ji G, Li J. STEAP2 is down-regulated in breast cancer tissue and suppresses PI3K/AKT signaling and breast cancer cell invasion in vitro and in vivo. Cancer Biol Ther. 2020;21:278–91.
8. Korkmaz CG, Korkmaz KS, Kurys P, Elbi C, Wang L, Klokk TI, Hammarstrom C, Troen G, Svindland A, Hager GL, Saatcioglu F. Molecular cloning and characterization of STAMP2, an androgen-regulated six transmembrane protein that is overexpressed in prostate cancer. Oncogene. 2005;24:4934–45.
9. Hubert RS, Vivanco I, Chen E, Rastegar S, Leong K, Mitchell SC, Madraswala R, Zhou Y, Kuo J, Raitano AB, Jakobovits A, Saffran DC, Afar DE. STEAP: a prostate-specific cell-surface antigen highly expressed in human prostate tumors. Proc Natl Acad Sci U S A. 1999;96:14523–8.
10. Ohgami RS, Campagna DR, McDonald A, Fleming MD. The Steap proteins are metalloreductases. Blood. 2006;108:1388–94.
11. Arner P, Stenson BM, Dungner E, Näslund E, Hoffstedt J, Ryden M, Dahlman I. Expression of six transmembrane protein of prostate 2 in human adipose tissue associates with adiposity and insulin resistance. J Clin Endocrinol Metab. 2008;93:2249–54.
12. Gomes IM, Maia CJ, Santos CR. STEAP proteins: from structure to applications in cancer therapy. Mol Cancer Res. 2012;10:573–87.
13. Qin DN, Kou CZ, Ni YH, Zhang CM, Zhu JG, Zhu C, Wang YP, Zhu GZ, Shi C, Ji CB, Guo XR. Monoclonal antibody to the six-transmembrane epithelial antigen of prostate 4 promotes apoptosis and inhibits proliferation and glucose uptake in human adipocytes. Int J Mol Med. 2010;26:803–11.
14. Chen X, Zhu C, Ji C, Zhao Y, Zhang C, Chen F, Gao C, Zhu J, Qian L, Guo X. STEAP4, a gene associated with insulin sensitivity, is regulated by several adipokines in human adipocytes. Int J Mol Med. 2010;25:361–7.
15. Liao Y, Zhao J, Bulek K, Tang F, Chen X, Cai G, Jia S, Fox PL, Huang E, Pizarro TT, Kalady MF, Jackson MW, Bao S, Sen GC, Stark GR, Chang CJ, Li X. Inflammation mobilizes copper metabolism to promote colon tumorigenesis via an IL-17-STEAP4-XIAP axis. Nat Commun. 2020;11:900.
16. Jin Y, Wang L, Qu S, Sheng X, Kristian A, Mælandsmo GM, Pällmann N, Yuca E, Tekedereli I, Gorgulu K, Alpay N, Sood A, Lopez-Berestein G, Fazli L, Rennie P, Risberg B, Wæhre H, Danielsen HE, Ozpolat B, Saatcioglu F. STAMP2 increases oxidative stress and is critical for prostate cancer. EMBO Mol Med. 2015;7:315–31.
17. Wu HT, Chen WJ, Xu Y, Shen JX, Chen WT, Liu J. The tumor suppressive roles and prognostic values of STEAP family members in breast cancer. Biomed Res Int. 2020;2020:9578484.
18. Wu HC, Yang HI, Wang Q, Chen CJ, Santella RM. Plasma DNA methylation marker and hepatocellular carcinoma risk prediction model for the general population. Carcinogenesis. 2017;38:1021–8.
19. Yan D, Dong W, He Q, Yang M, Huang L, Kong J, Qin H, Lin T, Huang J. Circular RNA circPICALM sponges miR-1265 to inhibit bladder cancer metastasis and influence FAK phosphorylation. EBioMedicine. 2019;48:316–31.
20. Ju MH, Jang EJ, Kang SH, Roh YH, Jeong JS, Han SH. Six-transmembrane epithelial antigen of prostate 4: an indicator of prognosis and tumor immunity in hepatocellular carcinoma. JHC. 2023;10:643–58.
21. Xie B, Zhong B, Zhao Z, Hu J, Yang J, Xie Y, Zhang J, Long J, Yang X, Li H. STEAP4 inhibits cisplatin-induced chemotherapy resistance through suppressing PI3K/AKT in hepatocellular carcinoma. Cancer & metabolism. 2023;11:26.
22. Suski JM, Braun M, Strmiska V, Sicinski P. Targeting cell-cycle machinery in cancer. Cancer Cell. 2021;39:759–78.
23. Sun J, Ji G, Xie J, Jiao Z, Zhang H, Chen J. Six-transmembrane epithelial antigen of the prostate 1 is associated with tumor invasion and migration in endometrial carcinomas. J Cell Biochem. 2019;120:11172–89.
24. Fu D, Zhang X, Zhou Y, Hu S. A novel prognostic signature and therapy guidance for hepatocellular carcinoma based on STEAP family. BMC Med Genomics. 2024;17:16.
25. Torrez CZ, Easley A, Bouamar H, Zheng G, Gu X, Yang J, Chiu YC, Chen Y, Halff GA, Cigarroa FG, Sun LZ. STEAP2 promotes hepatocellular carcinoma progression via increased copper levels and stress-activated MAP kinase activity. Sci Rep. 2024;14:12753.
26. Teyssot ML, Jarrousse AS, Chevry A, De Haze A, Beaudoin C, Manin M, Nolan SP, Diez-Gonzalez S, Morel L, Gautier A. Toxicity of copper(I)-NHC complexes against human tumor cells: induction of cell cycle arrest, apoptosis, and DNA cleavage. Chemistry. 2009;15:314–8.
27. Shimada K, Reznik E, Stokes ME, Krishnamoorthy L, Bos PH, Song Y, Quartararo CE, Pagano NC, Carpizo DR, deCarvalho AC, Lo DC, Stockwell BR. Copper-binding small molecule induces oxidative stress and cell-cycle

arrest in glioblastoma-patient-derived cells. Cell Chem Biol. 2018;25:585-594.e587.
28. Foo JB, Ng LS, Lim JH, Tan PX, Lor YZ, Loo JSE, Low ML, Chan LC, Beh CY, Leong SW, Saiful Yazan L, Tor YS, How CW. Induction of cell cycle arrest and apoptosis by copper complex Cu(SBCM)(2) towards oestrogen-receptor positive MCF-7 breast cancer cells. RSC Adv. 2019;9:18359–70.
29. Ruiz LM, Jensen EL, Rossel Y, Puas GI, Gonzalez-Ibanez AM, Bustos RI, Ferrick DA, Elorza AA. Non-cytotoxic copper overload boosts mitochondrial energy metabolism to modulate cell proliferation and differentiation in the human erythroleukemic cell line K562. Mitochondrion. 2016;29:18–30.
30. Bischoff ME, Shamsaei B, Yang J, Secic D, Vemuri B, Reisz JA, D'Alessandro A, Bartolacci C, Adamczak R, Schmidt L, Wang J, Martines A, Venkat J, Toffessi Tcheuyap V, Biesiada J, Behrmann CA, Vest KE, Brugarolas J, Scaglioni PP, Plas DR, Patra KC, Gulati S, Landero Figueroa JA, Meller J, Cunningham JT, and Czyzyk-Krzeska MF. Copper drives remodeling of metabolic state and progression of clear cell renal cell carcinoma. Cancer Discov 2024. doi: 10.1158/2159-8290.CD-24-0187.
31. Turski ML, Thiele DJ. New roles for copper metabolism in cell proliferation, signaling, and disease. J Biol Chem. 2009;284:717–21.
32. Knutson MD. Steap proteins: implications for iron and copper metabolism. Nutr Rev. 2007;65:335–40.
33. Lutsenko S, Roy S, and Tsvetkov P. Mammalian copper homeostasis: physiologic roles and molecular mechanisms. Physiol Rev. 2025;105:441-491.
34. Llovet JM, Ricci S, Mazzaferro V, Hilgard P, Gane E, Blanc JF, de Oliveira AC, Santoro A, Raoul JL, Forner A, Schwartz M, Porta C, Zeuzem S, Bolondi L, Greten TF, Galle PR, Seitz JF, Borbath I, Haussinger D, Giannaris T, Shan M, Moscovici M, Voliotis D, Bruix J, and Group SIS. Sorafenib in advanced hepatocellular carcinoma. N Engl J Med. 2008;359:378-390.
35. Jiang C, Wu B, Xue M, Lin J, Hu Z, Nie X, Cai G. Inflammation accelerates copper-mediated cytotoxicity through induction of six-transmembrane epithelial antigens of prostate 4 expression. Immunol Cell Biol. 2020;99:392–402.
36. Weisberg SP, McCann D, Desai M, Rosenbaum M, Leibel RL, Ferrante AW. Obesity is associated with macrophage accumulation in adipose tissue. J Clin Investig. 2003;112:1796–808.
37. Pihlstrom N, Jin Y, Nenseth Z, Kuzu OF, Saatcioglu F. STAMP2 expression mediated by cytokines attenuates their growth-limiting effects in prostate cancer cells. Cancers. 2021;13:1579.
38. Xue X, Bredell BX, Anderson ER, Martin A, Mays C, Nagao-Kitamoto H, Huang S, Győrffy B, Greenson JK, Hardiman K, Spence JR, Kamada N, Shah YM. Quantitative proteomics identifies STEAP4 as a critical regulator of mitochondrial dysfunction linking inflammation and colon cancer. Proc Natl Acad Sci USA. 2017;114:E9608-e9617.
39. Orfanou I-M, Argyros O, Papapetropoulos A, Tseleni-Balafouta S, Vougas K, Tamvakopoulos C. Discovery and pharmacological evaluation of STEAP4 as a novel target for HER2 overexpressing breast cancer. Front Oncol. 2021;11:608201
40. Barr FA, Sillje HH, Nigg EA. Polo-like kinases and the orchestration of cell division. Nat Rev Mol Cell Biol. 2004;5:429–40.
41. Wang XQ, Zhu YQ, Lui KS, Cai Q, Lu P, Poon RT. Aberrant Polo-like kinase 1-Cdc25A pathway in metastatic hepatocellular carcinoma. Clin Cancer Res. 2008;14:6813–20.
42. Li L, Huang K, Zhao H, Chen B, Ye Q, Yue J. CDK1-PLK1/SGOL2/ANLN pathway mediating abnormal cell division in cell cycle may be a critical process in hepatocellular carcinoma. Cell Cycle. 2020;19:1236–52.
43. Pellegrino R, Calvisi DF, Ladu S, Ehemann V, Staniscia T, Evert M, Dombrowski F, Schirmacher P, Longerich T. Oncogenic and tumor suppressive roles of polo-like kinases in human hepatocellular carcinoma. Hepatology. 2010;51:857–68.
44. Smith J, Tho LM, Xu N, Gillespie DA. The ATM-Chk2 and ATR-Chk1 pathways in DNA damage signaling and cancer. Adv Cancer Res. 2010;108:73–112.
45. Flynn RL, Zou L. ATR: a master conductor of cellular responses to DNA replication stress. Trends Biochem Sci. 2011;36:133–40.
46. Abdel-Fatah TM, Middleton FK, Arora A, Agarwal D, Chen T, Moseley PM, Perry C, Doherty R, Chan S, Green AR, Rakha E, Ball G, Ellis IO, Curtin NJ, Madhusudan S. Untangling the ATR-CHEK1 network for prognostication, prediction and therapeutic target validation in breast cancer. Mol Oncol. 2015;9:569–85.
47. Parikh RA, Appleman LJ, Bauman JE, Sankunny M, Lewis DW, Vlad A, Gollin SM. Upregulation of the ATR-CHEK1 pathway in oral squamous cell carcinomas. Genes Chromosomes Cancer. 2014;53:25–37.
48. Hou Y, Allan LA, Clarke PR. Phosphorylation of XIAP by CDK1-cyclin-B1 controls mitotic cell death. J Cell Sci. 2017;130:502–11.
49. Chen WJ, Wu HT, Li CL, Lin YK, Fang ZX, Lin WT, Liu J. Regulatory roles of six-transmembrane epithelial antigen of the prostate family members in the occurrence and development of malignant tumors. Front Cell Dev Biol. 2021;9:752426.
50. Che Y, Ye F, Xu R, Qing H, Wang X, Yin F, Cui M, Burstein D, Jiang B, Zhang DY. Co-expression of XIAP and cyclin D1 complex correlates with a poor prognosis in patients with hepatocellular carcinoma. Am J Pathol. 2012;180:1798–807.

Publisher's Note